A.Yu.Ivanov, V.I.Nedolugov, S.V.Vasiliev

Fast holographic filming of laser plasma evolution in electric field

Grodno State University, Ozheshko 22, 230023 Grodno, Belarus,
Phone 0152-484042, e-mail: ion_ne@mail.ru

A two-wavelength high-speed holographic cinematography, integral and time-resolved spectroscopy and splite unfolding methods were used in an investigation of a laser plasma initiated at the surfaces of metal samples by laser pulses in the external electric field. The temporal evolution of the electron densities and heavy particle concentrations was determined and a study was made of the nature of motion of shock wave and plasma fronts. A weak dependence of the evolution of the shock wave velocity on the target materials (aluminum, copper, zinc, led, indium) was observed in the average power density range ($10^6 - 10^7$W/cm^2). A faster increase in the dimensions of a refracting plasma region, compared to a luminous region, and strong expulsion of cold air by an erosion plasma were recorded.

Our aim was to investigate the temporal evolution of the distributions of the electron density and of the concentration of heavy particles in the plasma plume appearing near the surface of the metal sample irradiated by the laser beam with the average power density range ($10^6 - 10^7$W/cm^2).

The scheme of the experimental setup used in the study is presented in Fig. 1. The radiation of the GOR-100M ruby laser *(1)* *(λ =0.694 μm)* operating in the free oscillation regime (pulse duration $\tau \sim 1.2$ ms, Fig. 2) or rhodamine laser *(λ =0.58 μm)*, pulse duration $\tau \sim 20$ μs) passed through the focusing system *(2)* and was directed through the hole in the electrode *(3)* onto the sample *(4)* that served as the second electrode and was mounted in air at a pressure of 10^5 Pa.
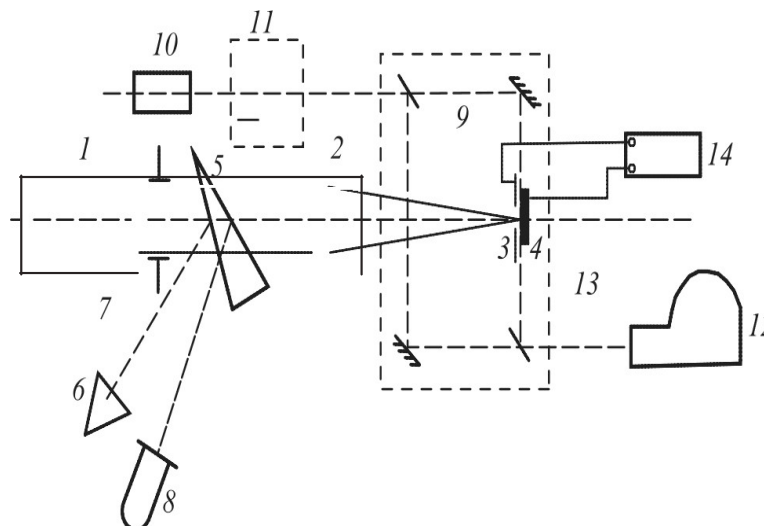

Figure 1. The experimental setup schematic diagram.

The radiation spot diameter with sharp edges on the sample was varied in the course of the experiments from 1 to 2 mm. From the front face of the

glass wedge *(5)* a part (4%) of laser radiation was directed into the IMO-2N energy meter (6), whose entrance window was located in the focal plane of the lens (7). The energy of the laser pulses varied from 5 to 60 J. The FEK-14 coaxial photodetector *(8),* the signal from which was coupled to the S8-13 oscilloscope, was used to record the temporal shape of the laser pulse. The voltage was applied to the electrodes *(3, 4)* from the source *(14),* built on the basis of the UN 9/27-13 voltage multiplier of the TVS-110 unit. The source allowed the voltage variation within 25 kV and its stabilization in the course of the experiment.
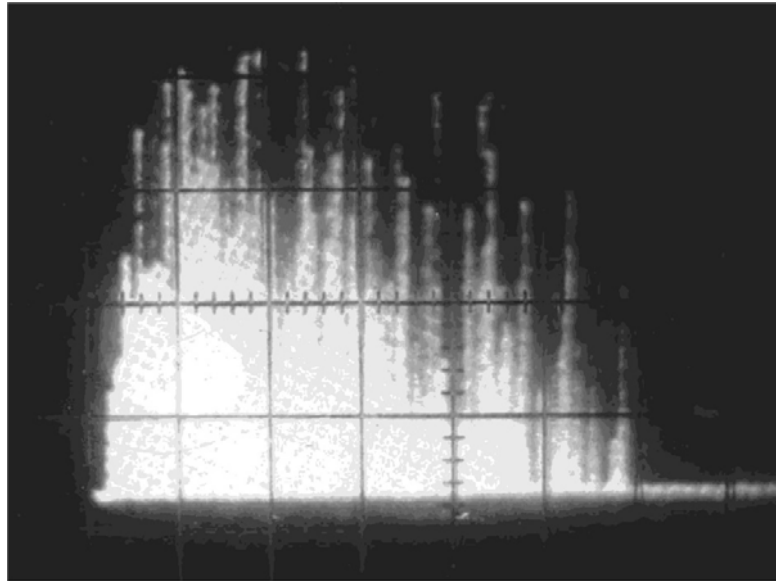

Figure 2. Radiation pulse from the GOR-100M laser oscillogram.
The scanning rate is $200 \, \mu s$/div.

To study the spatial and temporal evolution of the laser plasma plume in the course of laser radiation action on the sample, we used the method of high-speed holographic motion-picture recording. The interelectrode gap was placed in one of the arms of a Mach-Zehnder interferometer (9), which was illuminated with the radiation of the ruby laser *(10)* ($\lambda = 0.694 \, \mu m$) operating in the free oscillation regime. The pulse duration of the radiation amounted to $\sim 400 \, \mu s$. The transverse mode selection in the probing laser was accomplished using the aperture, placed in the cavity, and the longitudinal mode selection was provided by the Fabry-Perot cavity standard used as the output mirror. The probing radiation after the collimator *(11)* was a parallel light beam with the diameter up to 3 cm, which allowed observation of the steam-plasma cloud development.

The interferometer was attached to the SFR-1 M high-speed recording camera *(12),* in which the plane of the film was conjugate with the meridian section of the laser beam, acting on the sample, by means of the objective *(13).* The high-speed camera operated in the time magnifier regime. The described setup allowed recording of time-resolved holograms of the focused image of the laser plasma plume. Separate holographic frames provided temporal

resolution no worse than 0.8 μs (the single frame exposure time) and the spatial resolution in the object field ~ 50 μm. The error in the determination of the electron density was ~ 10% and it was governed by the precision with which the shifts of the fringes could be determined in the photographically developed interference patterns.

The diffraction efficiency of the holograms allowed one to reconstruct and record interference and shadow pictures of the studied process under the stationary conditions. The shadow method was most sensitive to grad n, so that the nature of the motion of the front of a shock wave outside the laser plasma and of the motion of the plasma jet could be determined from the reconstructed shadow patterns. This gave information on the motion of the shock front and the laser plasma front generated at the surfaces of metal samples. It was found that the nature of the motion of the shock wave front was practically independent of the target material and was governed primarily by the average power density of the laser radiation.

The reconstructed interference patterns were used to determine the spatial and temporal distributions of the electron density in a laser plasma plume.

The reliability of the results obtained by the method of fast holographic cinematography was checked by determination of the velocity of the front of a luminous plasma jet by a traditional method using slit scans recorded with a second SFR-1M streak camera.

To study the surface shape of the crater that appears on the plate, we used the fringe projection method, which in the present case appeared to be more efficient than holographic methods of surface relief imaging and the stereophotogrammetric method, since, already at the stage of fringe projecting, it allowed obtaining a picture with controllable sensitivity of measurements and sufficiently good visibility of fringes, controlled visually. The sensitivity of measurements (relative fringe displacement) was set by changing the period of the projected fringes, and the good visibility was provided by changing the angle of illumination of the studied surface till removing the light flares from the crater surface. The present method is thoroughly described and successfully used in [1].

The optical scheme of the apparatus used to visualize the topography of crater is shown on Figure 2. Radiation of helium-neon laser *1* LGN-215 collimated by telescopic system *2* was used to illuminate Mach-Zehnder interferometer *3*. The interference picture was then projected to the sample *4* being studied. During the above procedure a system of dark and light strips was observed on the treated surface, and besides the configuration of strips was connected synonymously with the depth of the crater in the point of interference

$$h = d \cdot \Delta k / (tg\beta + tg\gamma).$$

Here d is a period of interference strips on the flat (nonirradiated) zone of the target, Δk – the displacement of a dark strip, β – an angle between the perpendicular to the surface of the irradiated sample and the projected interference surface, γ – an

angle between the normal to the surface of the irradiated sample and the optical axis of the photographic camera.

The sample surface was optically mated with the picture surface *5* with the help of the objective "Helios-44-2". Contour stripes on the picture surface were fixed on the photographic film.
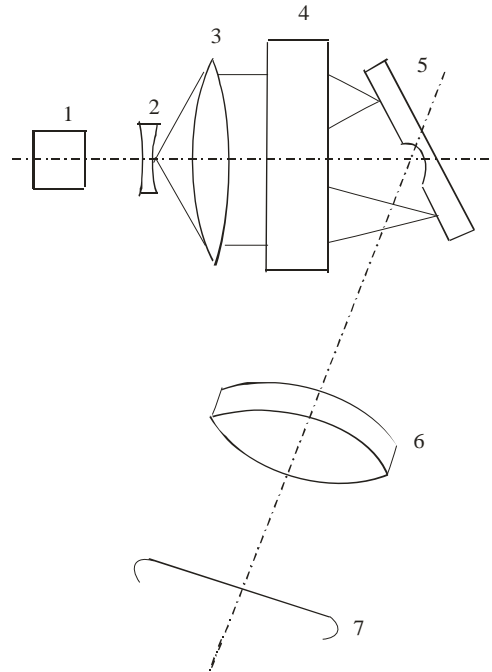

Figure 3. Schematic diagram of the visualization apparatus.

The experimental results have shown that at any polarity of the applied voltage [with positive or negative potential at the irradiated sample with respect to the electrode *(3)* the topography of the crater is practically identical and is determined by the energy distribution over the focusing spot of the laser radiation (Figs 4, 5).

а   *б*

Figure 4. Photographs of the craters obtained under the action of laser pulses on the target in the absence of the external electric field (a) and in the presence of the field (b).

Figures 6 a – c display the interferograms, reconstructed from the holograms recorded at different instants in the course of high-speed holographic motion-picture shooting. The figure clearly illustrates both the initial stage of the laser torch development and the plasma flow around the electrode *(3)* at different directions of the external electric field strength vector.

Figures 6 d – f represent the data on the distribution of concentration of free electrons in the plasma of an evaporated metal at different instants, obtained by processing the interferograms [2]. Although the energy distribution over the laser radiation focusing spot is not uniform, the lines of equal concentration are practically smooth, which is an evidence of relatively uniform ionization of the eroded substance steams. It is essential that, despite a substantial increase in the plasma formation over time, the mean electron concentration in the torch remains practically unchanged and even slightly grows, which may be associated both with a constant increase in the mass of emitted substance and with secondary ionization of the plasma by the laser radiation. Note, that the presence of an external electric field weakly affects the concentration of electrons in the laser plasma plume.
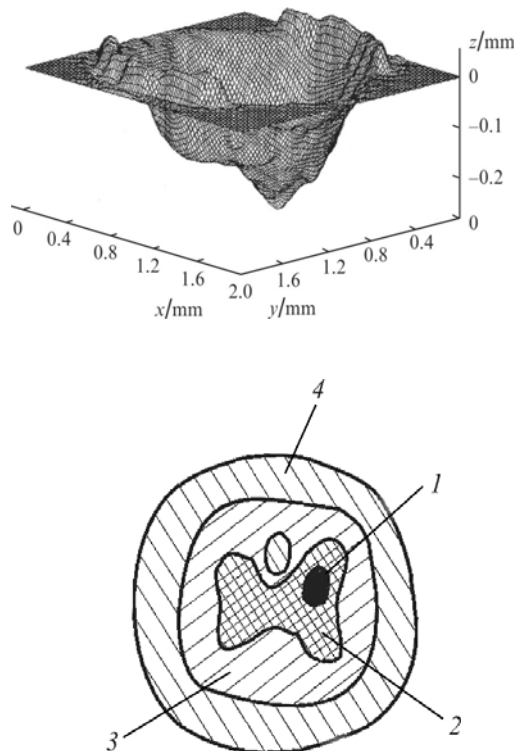

Figure 5. Volume topogram of a crater (a) and the distribution of light energy density over the transverse cross-section of the laser beam (b): 4.5 *(1)*, 3.5 *(2)*, 1.2 *(3)*, and 0.8 J mm^{-2} *(4)*.

When the interelectrode separation was 2 cm, the maximal transverse size of the steam-plasma cloud at the surface of the electrode *(3)* for negative

voltage on the target was 2 cm and in the absence of the external electric field it was *1.5* cm. This may be observed both in the interferograms and by the burn on the polyethylene film protecting the second electrode. As seen from interferograms, after reaching the second electrode in 56, 64, and 72 *μs*, respectively, the steam-plasma cloud practically does not grow in the transverse dimensions. Probably it is due to the flowing out of the plasma from the interelectrode gap through the hole in the electrode *(3),* which is used for passing the laser radiation to the target (the hole diameter being 1 cm).
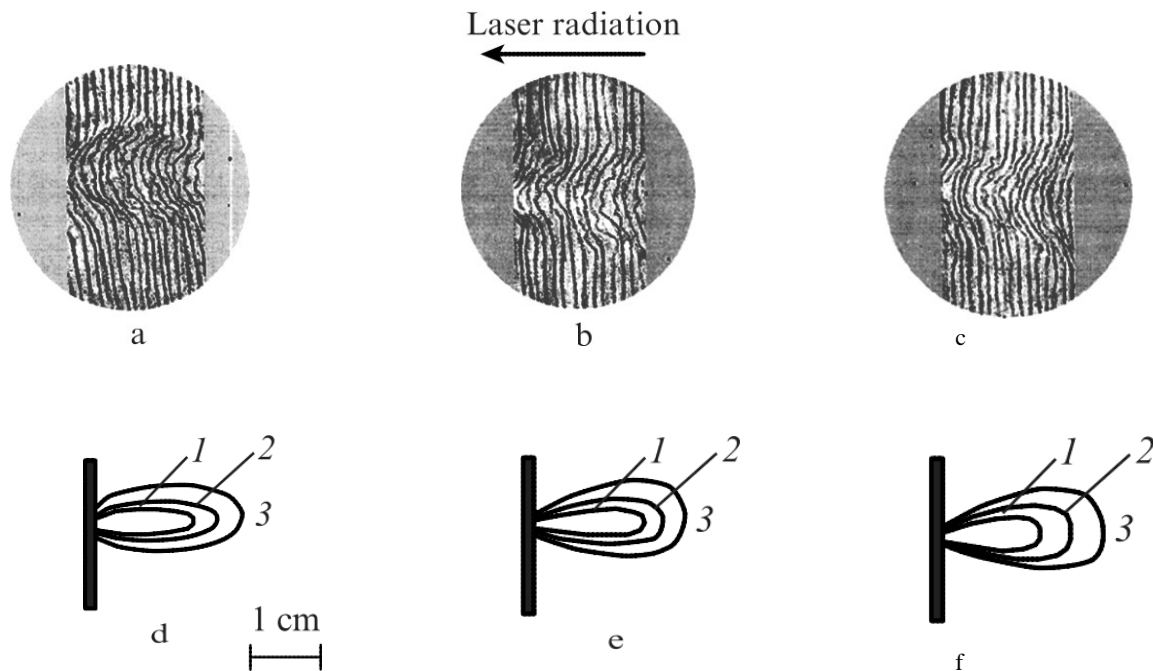

Figure 6. Interferograms of laser plasma torches (a, b, c) and electron concentration isolines in them (d, e, f) at the negative target potential (**b,** e) and at the positive target potential (c, f) at the instants 72 *μs* after the onset of the laser action; curve *(1)* corresponds to the electron concentration 5x 10^{18}, curve *(2)* to 2.5x 10^{18}, and curve *(3)* to 10^{18} cm^{-3}.

Figure 7 presents the time dependences of the plasma pluime front motion velocity at different directions of the external electric field strength vector, calculated by using the information, obtained by analyzing the temporal variation of the interferograms. It is seen that even when the plasma front reaches the electrode (3), its velocity not only does not decrease (which is typical for late stages of the laser plasma torch existence [3]), but even increases; this happens both in the presence of the external electric field of any orientation and in the absence of the field. As already mentioned, this is due to the permanent and significant increase in the mass of the material, carried out under the action of laser radiation on the irradiated sample, as well as to the secondary ionization of plasma by laser radiation.

The maximal expansion velocity of the plasma torch amounted to 350 m/s for the negative voltage at the target, 310 m/s in the absence of the external electric field, and 270 m/s for the positive voltage applied to the target.

Our investigation showed that the time evolution of the leading edge of a luminous plasma moving away from the surface of a sample, deduced from the slit scans, differed from the time evolution of the front of the plasma jet, which was recorded by the shadow method. This allowed us to conclude that the concentration of the heavy particles, responsible for the radiation emitted by the plasma, was low at the front of the laser plasma jet, whereas the electron density was sufficient for reliable determination of the contribution of electrons to refraction in a hologram.
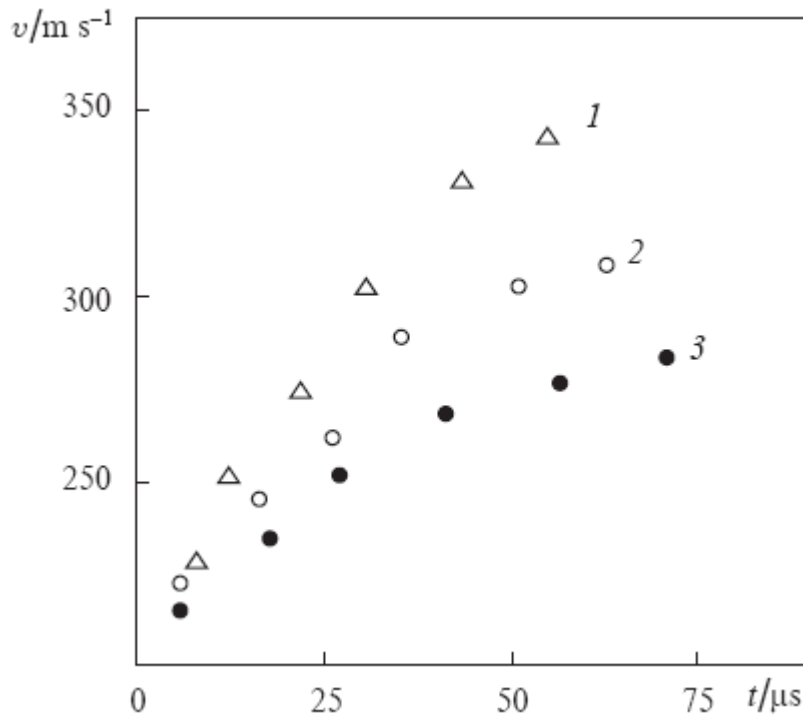

Figure 7. Time dependences of the velocity of the plasma torch front motion at the negative target potential *(1)*, in the absence of the field *(2)*, and at the positive target potential *(3)*.

The distribution of the density of cold air was determined and the electron density distribution was refined by two-wavelength holographic cinematography. We supplemented the system shown schematically in Fig. 1 with a second probe laser and an SFR-1M camera which recorded holograms at the wavelength of the radiation emitted by this laser. The second source of probe radiation was a laser utilizing a rhodamine 6G solution excited by a coaxial flashlamp. The use of a standard power supply system from a GOR-100M laser made it possible to generate output radiation pulses of $30 - 40$ μs duration. The line width was reduced employing a plane-parallel Fabry-Perot interferometer. This made it possible to obtain scan holograms of the process at $\lambda_1 = 0.69$ μm and $\lambda_2 = 0.58$ μm, and to separate the contribution of electrons from that of heavy particles to the refraction of a plasma jet.

This two-wavelength holographic cinematography method was used to determine the radial distributions of the electron density and of the heavy-particle

concentration at different moments in time and for different sections of laser plasma near the irradiated surface of an irradiated sample

At distances of 10 – 15 mm from the surface of a sample it was found that heavy particles ("hot" atoms and ions) of metals and molecules of atmospheric gases made only a small contribution to refraction. At large distances (where there were no "heated" luminous particles) the contribution of the cold dense air became significant. This was due to the pushing out of air by a plasma cloud.

In accordance with the results presented above, the dynamics of the processes on the surface of a sample, placed in an external electric field with the strength from 0 to 10^6 V m^{-1} and subject to the action of the pulsed laser radiation with the parameters mentioned above, is thought to be the following. The primary plasma formation and the initial stage of the laser torch development, in principle, do not differ from those observed in the absence of the external electric field. The metal is melted and evaporated. As a result of local formation of steam and plasma [4, 5], the erosion torch begins to form with the fine-dispersed liquid-droplets phase. Note, that the bulk evaporation is promoted by the gases, diluted in the metal, and by the spatiotemporal nonuniformity of the laser radiation [4]. At a radiation flux density $10^6 – 10^7$ W cm^2 the bulk evaporation is typical of all metals used in the experiments [5]. Obviously, the presence of the external electric field affects (increases or decreases depending on the direction of the field strength vector) the velocity of motion of the plasma front and causes some distortion of the plasma cloud shape. It is essential that the mentioned differences (at the considered parameters of laser radiation) are observed only at the initial stage of the laser plume development, because after the steam-plasma cloud reaches the electrode *(3)* an electric breakdown (short-circuit) occurs, and the external field in the interelectrode gap disappears.

REFERENCES

1. Bosak NA., Vasil'ev S.V., Ivanov A.Yu., Min'ko L.Ya., Nedolugov VI., Chumakov A.N. *Kvantovaya Elektron.,* 27, 69 (1999) *[Quantum Elelctron., 29, 69 (1999)].*
2. Ivanov A.Yu. Acoustic diagnostics of materials laser treating process. Grodno: GrSU, 2007.
3. Barikhin B.A., Ivanov A.Yu., Nedolugov VI. *Kvantovaya Elektron.,* 17, 1477 (1990) *[Soy. J. Quantum Electron., 20, 1386 (1990)].*
4. Goncharov V.K., Kontsovoy V.L., Puzyrev MV. *Inzhenerno- JIzicheskii zhurnal,* 66, 662 (1994) *[Journal of Engineering Physics and Thermophysics,* **66,** 588 (1994)].
5. Goncharov V.K., Kontsevoy V.L., Puzyrev MV. *Kvantovaya Elektron.,* 22, 249 (1995) *[Quantum Elelctron., 25, 232 (1995)].*